Highly Concentrated Solar Radiation Measurement by means of an Inverse Method

L. Mongibello[*1], N. Bianco[2], R. Fucci[1], and F. Moscariello[2]
[1]ENEA – Italian National Agency for New Technologies, Energy and Sustainable Economic Development, CR Portici
[2]Università di Napoli Federico II, Dipartimento di Energetica, Termofluidodinamica applicata e Condizionamenti ambientali (DETEC)
[*] postal address: ENEA Portici RC, P.le E. Fermi, 80055, Portici (NA), Italy; e-mail: luigi.mongibello@enea.it

Abstract: This work focuses on the numerical analysis conducted on the prototype sensor for the measurement of highly concentrated radiative heat fluxes, based on an inverse heat transfer method, realized at the ENEA Portici Research Center in collaboration with the DETEC department of the University of Naples Federico II.
The estimates of highly concentrated radiative heat fluxes on the target surface of the sensor are obtained by implementing the inverse heat transfer method based on the Levenberg-Marquardt algorithm, which permits to compute the radiative boundary condition on the exposed surface of the target by means of temperature measurements on the hidden bottom surface of the target.
As concerns the numerical analysis, a number of simulations have been carried out in order to evaluate the incidence of some characteristics relative both to the target exposed surface and the temperature measurements on the estimate of the concentrated radiative heat flux coming from the resolution of the inverse problem, namely the emissivity of the target surface of the sensor, the synchronization error in the temperature measurements, and the measurement error of the thermocouples. Indeed, the unsteady temperatures field inside the prototype has been simulated using the Comsol 2D axisymmetric solver, while the implementation of the inverse method algorithm has been performed using a home code written in Matlab.
In this work the numerical procedure implemented for the resolution of the inverse problem is detailed, and the results of the numerical analysis conducted on the prototype sensor are illustrated and analyzed. Furthermore, the results of experimental tests on the prototype sensor are reported and discussed.

Keywords: Inverse Heat Transfer Problem (IHTP), concentrated solar radiation, Comsol Multiphysics, Matlab.

1. Introduction

The great potential of solar energy and the necessity to operate with concentrated solar light systems in order to achieve high efficiencies have led to a very strong interest towards concentrated solar power (CSP) systems. At the ENEA Portici Research Centre, a 30kW of nominal radiative power solar furnace that consists of a heliostat equipped with flat mirrors and a parabolic concentrator with off-axis alignment is being installed. This system is capable to realize an average solar radiation concentration of about 2000 suns (2000 kW/m²) [1]. The energy flux relative to the concentrated radiation will be captured by a cavity receiver cooled with CO_2 and finally transferred to a user operating with high temperature energy (up to 850 °C), as for example a water splitting reactor for hydrogen production. Indeed, different currently available thermochemical cycles are characterized by working temperatures consistent with the above one, such as the iodine sulphur cycle [2] or the manganese ferrite cycle [3]. Furthermore, the solar furnace could be used to test a microturbine or a Stirling engine as well.
In the last few years, several studies have been addressed to the determination of highly concentrated radiative heat fluxes by means of the resolution of inverse heat transfer problems (IHCP) [4-10]. Moreover, IHCP are solved in order to estimate temperature dependent thermal properties of materials [11-13].
In a generic heat transfer problem relative to a solid object, the implementation of an inverse method permits to compute the boundary conditions, as well as the material thermophysical properties as a function of temperature, by means of temperature measurements realized inside the solid object or on its external surface. Inverse heat transfer methods (IHTM) are essentially iterative numerical procedures that use optimization algorithms in order to determine a reasonable estimate of a physical quantity, which in the present work is represented by the radiative heat flux, by means of the minimization of an objective function, which in this case corresponds to the difference between the experimental temperatures and the numerically calculated ones.
In this work the Levenberg-Marquardt algorithm [14] implemented numerically for the resolution of the inverse problem is detailed, and the results of the numerical analysis conducted on the prototype sensor are illustrated and analyzed. Figure 1 shows a picture of the prototype

sensor. It consists of a metallic disc, made of AISI 316 stainless steel, whose exposed surface represents the target of the concentrated radiative heat flux, a zirconia thermal insulating support, and a metallic support. Three K thermocouples are placed on the bottom hidden surface of the target for the temperature measurements.
Subsequently, the results of experimental tests on the prototype sensor are reported and discussed.

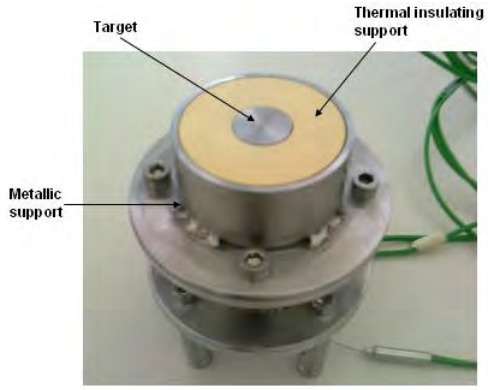

Fig. 1. Highly concentrated radiative heat flux prototype sensor.

2. Inverse heat transfer problem resolution procedure

Figure 2 shows the block diagram relative to the procedure used for the estimation of the concentrated radiative heat flux.

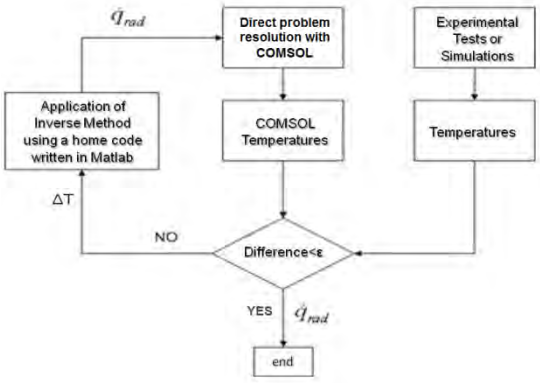

Fig. 2. Block diagram of the resolution of the inverse problem.

The implementation of the inverse method, based on the algorithm of Levenberg Marquardt, for the estimation of the concentrated radiative heat flux was performed using a home-made Matlab code. This procedure prescribes the iterative resolution of the direct problem performed using the COMSOL simulator. Figure 3 shows a sketch of the 2D axisymmetric computational domain relative to the numerical simulation of the sensor. As regards the initial temperature of the whole system, it depends on the environmental conditions in which the experimental tests are carried out. Relatively to the boundary conditions, a parabolic in space incident heat flux is imposed on the target, and on the same surface as well as on the upper surface of the insulating base a free convection boundary condition is imposed [8]. The radiative properties of the target exposed surface are specified in the following sections.

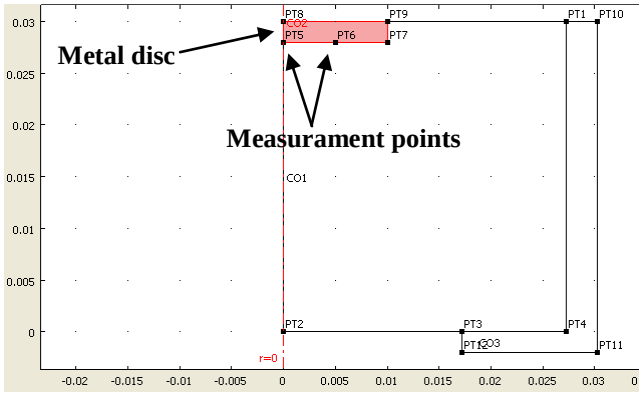

Fig. 3. Sketch of the 2D axisymmetric computational domain.

Figure 3 shows the two points on the hidden surface of the metal disc in which temperatures are numerically calculated and experimentally measured. One of these points is located on the symmetry axis, while the other point is located at a distance of 5 mm from the axis. The Comsol simulator solves the direct problem associated to the sensor in order to obtain the temperature values in the measuring points on the metal disc at certain instants of time. The simulation is initially performed starting from a tentative radiative heat flux. The calculated temperatures are then compared with those recorded during the experimental tests at the same instants. The difference between the computed and experimental temperatures are then used by the Matlab code to update the value of the radiative flux. Subsequently, a new resolution of the direct problem using the Comsol solver is made using the updated radiative heat flux, and so on. The loop terminates when the stop criterion is satisfied, i.e. when the norm of the difference between the calculated and experimental temperatures is relatively small.

3. Numerical analysis

The numerical analysis has been focused on the evaluation of the incidence of some characteristics relative both to the target exposed surface and the temperature measurements on the final estimate of the absorbed concentrated radiative heat flux coming from the resolution of the inverse problem, namely the emissivity of the target surface of the sensor, the synchronization error in the temperature measurements, and the measurement error of the thermocouples. In this numerical study the input temperatures to the inverse

problem are not measured experimentally, but they are obtained from the numerical simulation of the prototype sensor realized by means of the software Comsol Multiphysics 3.5a. Indeed, the above temperatures result from the unsteady numerical simulation of the prototype sensor considering an absorbed radiative heat flux constant in time and parabolic in space applied as a boundary condition on the target surface. In particular, two cases were analyzed with the absorbed heat flux of order 100 and 1000 kW/m^2, and a radius of the spot equal to 10 mm and 3 mm, respectively. The total absorbed power is 30W in both cases. Figures 4 and 5 show the temperature maps resulting from the simulations. In both the cases the emissivity ε of the target surface is fixed and equal to 0.9.

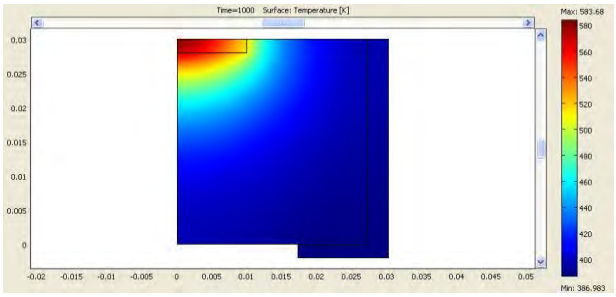

Fig. 4. Temperature map in the case with the absorbed heat flux of order 100 kW/m^2 after 1000 s.

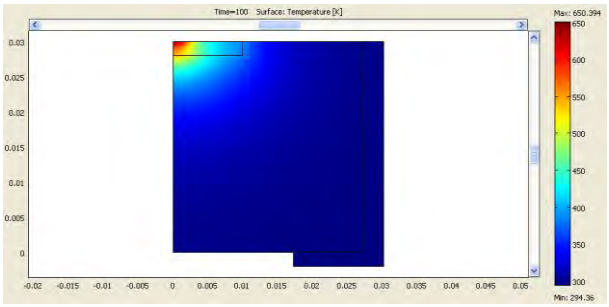

Fig. 5. Temperature map in the case with the absorbed heat flux of order 1000 kW/m^2 after 100 s.

3.1 Sensor estimation errors due to the uncertainty on the emissivity of the target surface

With reference to the block diagram in figure 2, the evaluation of the sensor estimation errors due to the uncertainty about the target surface emissivity has been realized using different values of the emissivity ε in the numerical simulations which provide the input temperatures to the inverse problem, whereas in the numerical resolution of the inverse problem the emissivity is fixed to 0.9. Figures 6 and 7 show a comparison between the spatial distributions of the heat flux estimated by means of the resolution of the inverse problem and those assigned in the numerical simulations with a Δε of 5%, while figures 8 and 9 refer to the simulations with Δε equal to 10%.

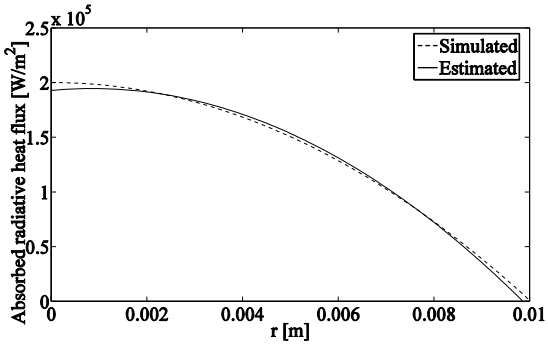

Fig. 6. Comparison between the simulated and the estimated heat flux with Δε=5% in the case with 100 kW/m^2.

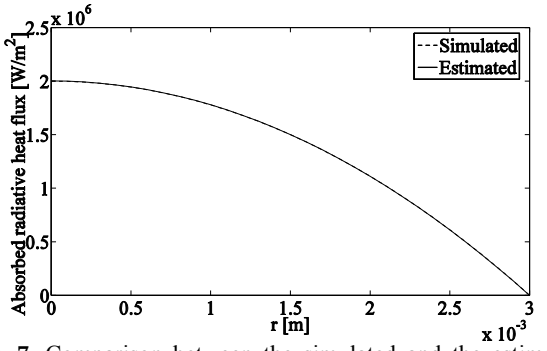

Fig. 7. Comparison between the simulated and the estimated heat flux with Δε=5% in the case with 1000 kW/m^2.

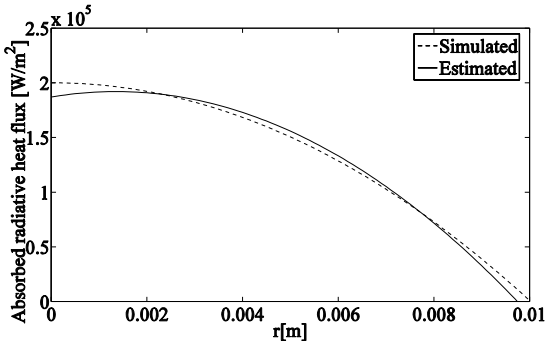

Fig. 8. Comparison between the simulated and the estimated heat flux with Δε=10% in the case with 100 kW/m^2.

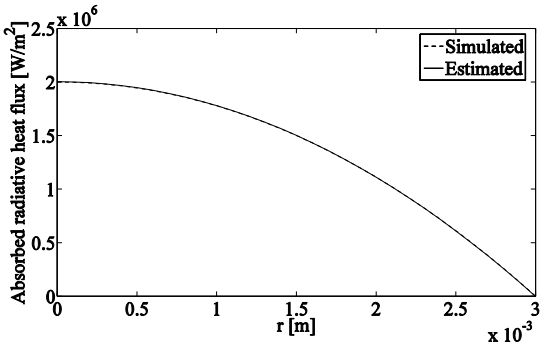

Fig. 9. Comparison between the simulated and the estimated heat flux with Δε=10% in the case with 1000 kW/m^2.

The results indicate that the estimated distributions of the heat fluxes resulting from the resolution of the inverse problems do not differ significantly from the ones assigned in the numerical simulations. In particular, in the cases with the average absorbed heat flux of order 1000 kW/m^2, the uncertainty due to the emissivity has no influence on the estimated heat flux. Finally, it can be stated that the incidence of the uncertainty relative to the value of the emissivity of the exposed surface of the target on the estimation of the absorbed radiative heat flux is negligible when the value of the heat flux is very high, i.e. when the solar radiation is highly concentrated.

3.2 Incidence of the synchronization errors on the sensor estimates

In this section the results of the numerical simulations conducted in order to evaluate the error in the sensor estimates caused by a bad synchronization are reported. Indeed, it has been considered a temporal gap between the time instants in which temperature measurements are done, that in the present numerical analysis correspond to the time instants in which temperatures are recorded in the simulations, and the ones relative to the input temperatures to the inverse problem. Figures 10 and 11 show a comparison between the estimated and the assigned heat flux in the case of a gap of one second.
The distributions show an higher error in the case with 1000 kW/m^2, due essentially to the higher temporal gradients of the temperature in the measurement points.

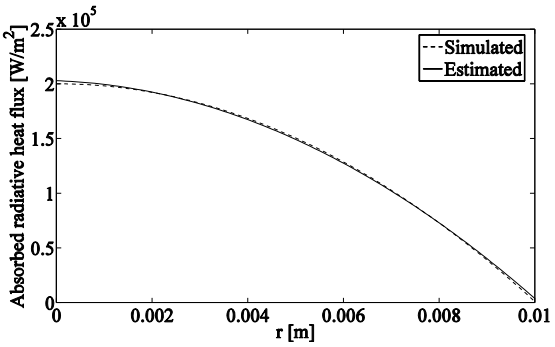

Figure 10. Incidence of a synchronization error of 1 s in the case with 100 kW/m^2.

Furthermore, with reference to figures 4 and 5 and considering the asymptotic behaviour of the target temperature field, the higher error in the case with 1000 kW/m^2 can be also related to the higher weight of the temporal gap with respect to the time instants in which temperatures are recorded, namely 10 and 90 seconds, and to the duration of the simulation (100 seconds), while in the case with 100 kW/m^2 the incidence of the synchronization error in the estimation of the heat flux is negligible due to the lower weight of the temporal gap with respect to the time instants in which temperatures are recorded, namely 100 and 900 seconds with a duration of the simulation of 1000 seconds.

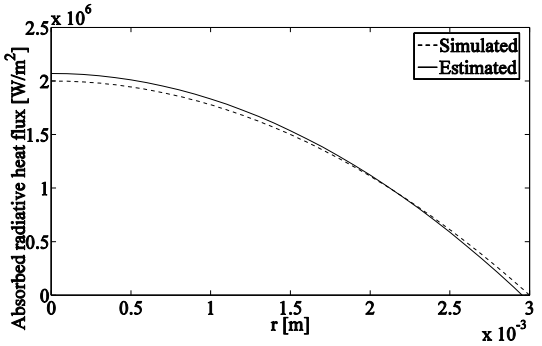

Figure 11. Incidence of a synchronization error of 1 s in the case with 1000 kW/m^2.

3.3 Incidence of the measurement error of the thermocouples on the sensor estimates

Finally, it has been evaluated the incidence of the maximum error relative to the temperature measurements, which is equal to 2.5°C when class II K thermocouples are used, on the determination of the absorbed radiative heat flux by means of the inverse method. The thermocouples error has been taken into account by adding the above error to the temperatures recorded in the numerical simulation, and then considering the resulting temperature values as input temperatures to the inverse problem.
Figures 12 and 13 show a comparison between the assigned and the estimated heat fluxes. It can be noticed a consistent difference between the two fluxes in the case with 100 kW/m^2, while in the case with 1000 kW/m^2 the difference is negligible. This is due to the higher weight of the above error with respect to the maximum temperature reached in the case with 100 kW/m^2.

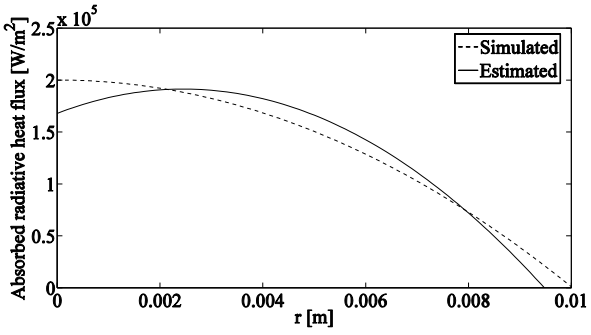

Figure 12. Incidence of thermocouples error in the case with 100 kW/m^2.

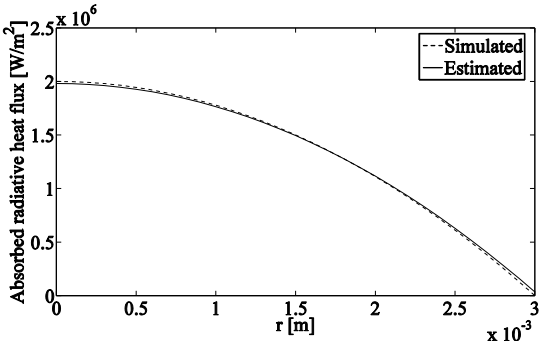

Figure 13. Incidence of thermocouples error in the case with 1000 kW/m^2.

4. Experimental tests

In this section the results of experimental tests on the prototype sensor realized using one of the CR ENEA Portici measuring stations will be reported and discussed. The test facility is showed in figure 14. It is composed by a two axis sun-tracker with two experimental sub-modules and a measurement circuit. The EKO STR-22 sun-tracker is provided with a sun-sensor and solar trajectory calculation algorithms which permit the achievement of a very precise accuracy (0,01°).

For the experimental analysis two square lenses of different types, namely a prismatic lens and a hybrid (prismatic-fresnel) one, were used in order to provide a concentrated solar radiation on the sensor target surface. The lenses have the same edge length (15.9 cm), and a averaged concentration factor in the measurement plane of about 200, with a spot of about 1.21 cm^2. Figures 15 and 16 show the spots of the two lenses detected using a CCD camera. It may be noticed that the prismatic lens produces a square-shaped spatial distributions of the concentrated radiation in the measurement plane, while the hybrid one produces a nearly axisymmetric spot.

As regards the thermocouples used for the temperature measurements in the points on the hidden surface of the target, these are mineral insulated "K" type with a stainless steel AISI 310 probe whose section diameter is 0.5 mm. The data acquisition was done with the USB NI 9211.

Figure 17 shows the prototype sensor during an experimental test. In this case, the estimates of the radiative heat flux are obtained using the input temperatures recorded experimentally on the target hidden surface. Relatively to the radiative properties of the target exposed surface, the emissivity and adsorptivity have been considered to be equal and temperature dependent, and their values are those relative to the well-known polished AISI 316 steel.

Figures 18 and 19 show the spatial distributions of the radiative heat flux estimated by the sensor for the prismatic and the hybrid lens, respectively.

Figure 14. ENEA outdoor measuring station

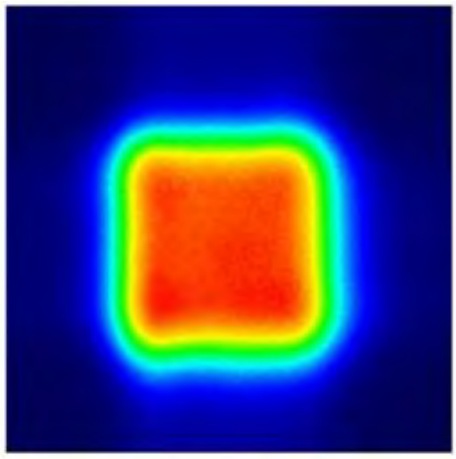

Figure 15. Light spot of the prismatic lens

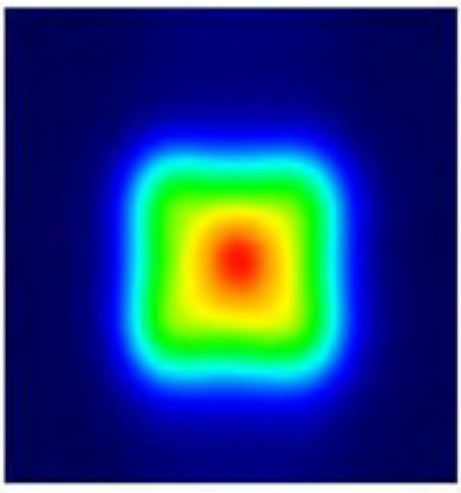

Figure 16. Light spot of the hybrid lens

Figure 17. Sensor housing

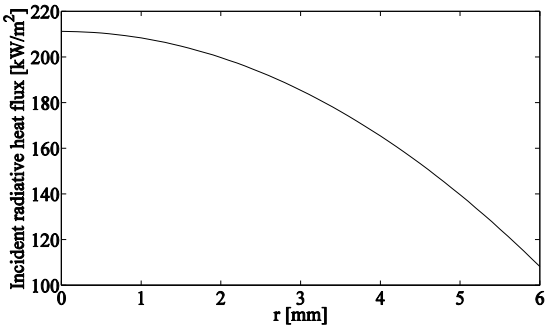

Figure 18. Concentrated radiative heat flux produced by the prismatic lens.

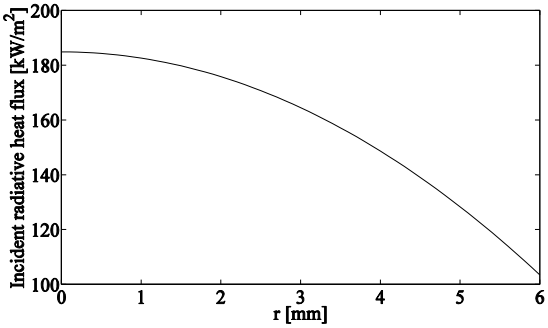

Figure 19. Concentrated radiative heat flux produced by the hybrid lens.

Table 1 reports for each of the two lenses the estimated and the experimental power on the target exposed surface. The above experimental power was calculated by measuring the direct solar radiation incident on the lens surface with a pyrheliometer (Hukseflux Pyrheliometer DR02). As can be clearly seen, the inverse method-based sensor produces a better estimate of the radiative power in the test realized using the hybrid lens. This is essentially due to the fact that the spot produced by the hybrid lens is nearly axisymmetric, which represents a necessary conditions for the 2D axisymmetric solver of the inverse problem.

Table 1. Estimated and experimental power.

	Acquisition instants [s]	Estimated power [W]	Experimental power [W]
Test 1 (prismatic lens)	100, 200	18.046	13.26
Test 2 (hybrid lens)	100, 200	12.23	12.29

5. Conclusions

At ENEA Portici Research Center a prototype sensor for the measurement of highly concentrated radiative heat fluxes, based on an inverse heat transfer method, has been analyzed numerically and tested experimentally in collaboration with the DETEC department of the University of Naples Federico II. The estimates of highly concentrated radiative heat fluxes on the target surface of the sensor are obtained by implementing the inverse heat transfer method based on the Levenberg-Marquardt algorithm, which permits to compute the radiative boundary condition on the exposed surface of the target by means of temperature measurements on the hidden bottom surface of the target performed using three type "K" thermocouples.

As concerns the numerical analysis realized by means of the softwares Comsol Multiphysics 3.5a and Matlab 7, it was found that, in the case of highly contentrated radiative heat fluxes of order 1000 suns, the prototype sensor is not very sensitive to the uncertainty related both to the value of the emissivity of the exposed surface of the target, and to the temperature measurements of the thermocouples. Furthermore, it emerged that the prototype works good also in the estimation of radiative heat fluxes with a lower concentration (100 suns) when synchronization errors are present.

Finally, the results of the experimental analysis were reported and discussed. These results confirmed the consistency of the technique implemented for the estimation of highly concentrated radiative heat fluxes.

6. References

[1] Contento, G., Cancro, and C., Privato, C., Layout and optical configuration of the ELIOSLAB project solar furnace, *ASME-ATI-UIT 2010 Conference on Thermal and Environmental Issues in Energy Systems*, Sorrento, Italy, May 16-19, 2010.

[2] Goldstein, S., Borgard, J., and Vitart, X., Upper bound and best estimate of the efficiency of the iodine sulphur cycle, *International Journal of Hydrogen Energy*, 2005, **30**, 619 - 626.

[3] Alvania, C., La Barbera, A., Ennas, G., Padella, F., and Varsano, F., Hydrogen production by using manganese ferrite: Evidences and benefits

of a multi-step reaction mechanism, *International Journal of Hydrogen Energy*, 2006, **31**, 2217-2222.

[4] Jianhua Zhou, Yuwen Zhang, J.K. Chen, Z.C. Feng, Inverse estimation of spatially and temporally varying heating boundary conditions of a two-dimensional object, *International Journal of Thermal Sciences,* Vol. 49, pp.1669-1679, (2010)

[5] Jianhua Zhou, Yuwen Zhang, J.K. Chen, Z.C. Feng, Inverse estimation of surface heating condition in a three-dimensional object using conjugate gradient method, *International Journal of Heat and Mass Transfer*, Vol.53, pp. 2643–2654, (2010)

[6] Harles F. Weber, Analysis and solution of the ill-posed inverse heat conduction problem, *International Journal of Heat and Mass Transfer*, Vol. 24, No.11, pp.1783-1792, (1981)

[7] Jan Taler, Theory of transient experimental techniques for surface heat transfer, *International Journal of Heat and Mass Transfer*, Vol. 39, No.17, pp 3733-3748, (1996)

[8] P. Le Bideau, J.P. Ploteau, P. Glouannec, Heat flux estimation in an infrared experimental furnace using an inverse method, *Applied Thermal Engineering*, Vol.29 pp. 2977–2982, (2009)

[9] J. Ballestrìn, C. A. Estrada, M. Rodrıguez-Alonso, C. Perez-Rabago, L.W. Langley and A. Barnes, High-heat-flux sensor calibration using calorimetry, *Metrologia* 41, pp. 314–318, (2005)

[10] R. Fucci, N. Bianco, L. Mongibello, A. Parretta, C. Privato, Spatial and spectral distribution determination of solar light concentrated by solar collectors, *26th European Photovoltaic Solar Energy Conference and Exhibition*.

[11] B. Sawaf, M. N. Ozisik, An inverse analysis to estimate linearly temperature dependent thermal conductivity components and heat capacity of an orthotropic medium, *International Journal of Heat and Mass Transfer*, Vol. 38, No.16, pp.3005–3010, (1995)

[12] F.A. Rodrigues, H.R.B. Orlande, M.M. Mejias, Use of a single heated surface for the estimation of thermal conductivity components of orthotropic 3D solids, *Inverse Problems in Science and Engineering*, Vol.12, No.5, pp. 501–517, October (2004)

[13] S.S. Sablani, A. Kacimov, J. Perret, A.S. Mujumdar, A. Campo, Non-iterative estimation of heat transfer coefficients using artificial neural network models, *International Journal of Heat and Mass Transfer*, Vol. 48, pp.665–679, (2005)

[14] Ozisik, M.N., and Orlande, H.R.B., "Inverse Heat Transfer: Fundamentals and Applications", *Taylor & Francis*, New York, (2000).